Front. Optoelectron. China 2010, 3(4): 382–386
DOI 10.1007/s12200-010-0125-6

RESEARCH ARTICLE

Method of optical interference testing error separation

Yunpeng FENG[1], Xiaoyan QIAO[2], Haobo CHENG (✉)[1], Yongfu WEN[1], Ya GAO[1], Huijing ZHANG[1]

1 School of Optoelectronics, Beijing Institute of Technology, Beijing 100081, China
2 School of Electrical and Electronic Engineering, North China Electric Power University, Beijing 102206, China

Abstract During the testing of aspherical mirrors through the null compensation method, structural parameters observe changes which affect the test results of interference pattern. Several errors are induced due to the maladjustment among compensator, interferometer and the mirror under test. It is important for optical manufacturing, testing and the actual alignment process to distinguish between the aberrations arising from both surface errors and maladjustment of the null compensation testing system. The purpose of this paper is to obtain the real aspheric surface errors during the optical polishing process. In this work, we have established an error separation model to the least square method to separate the errors caused by the maladjustment of the testing system from the test results. Finally, the analysis and simulation results show that high precision figure errors can be obtained by separating the maladjustment errors.

Keywords aspheric mirror, interferometric testing, adjustment error, maladjustment, error separation

1 Introduction

When large aperture and complex optical components are tested with null compensation method, the testing system used is, generally, very complicated. During testing, the adjustment of compensator, interferometer and the optical element under test, may introduce some adjustment errors which, eventually, may reflect in the testing results [1]. The aberrations arising from maladjustment of the testing system must be separated in order to get actual surface errors of the testing optical surface, specifically, in the optical polishing stage. It is the pivotal technology of high-precision optical interferometry that distinguishes between the aberrations arising from surface errors and the aberrations arising from maladjustments of the testing system. The technology is significant in optical manufacturing process, to set the proper polishing parameters and the polishing path. If the testing system is adjusted manually, the adjusting precision is relatively low, and the period of adjustment is longer than done by the machine [2].

In order to obtain accurate surface errors of the aspheric mirror under test, the structural maladjustments and the algorithm for maladjustment solution are studied, based on optical aspheric interferometry. First, a mathematical model for the test results and maladjustments of testing system is established. Then the sensitivity matrix of the system structure is calculated and the adjustment errors are separated using least square method. Finally, the accurate surface errors of the mirror under test are obtained by structure adjustment [3].

Received September 11, 2010; accepted September 29, 2010

E-mail: h_cheng@yahoo.cn

2 Errors separation model

In the testing system, the design errors and machining errors of components are considered to be fixed, so the aberrations in the testing results are just concerned with the structural parameters of the testing system. If the relation between them can be found, the structural maladjustments can be solved correspondingly. Then the tested surface errors can be obtained through the fine adjustment of structural parameters [4,5].

Mathematically, the aberrations are the function of the structural parameters. $F_j, j = 1,2,...,m$, indicates the system aberrations. x_i, $i = 1,2,...,n$, indicates structural parameters of the testing system. Then the function is written as follows:

$$F_i = f_i(x_1,x_2,...,x_n), \quad i = 1,2,...,m, \tag{1}$$

where f_i, $i = 1,2,...,m$, is the function between aberrations and the structural parameters. It is a very complex nonlinear equation. Error separation, mathematically,

means establishing and solving this equation. In other words, to solve for the solutions $(x_1,x_2,...,x_n)$ according to the required image quality $(F_1,F_2,...,F_m)$, which are the structural parameters of the testing system we need.

Actually, due to the complexity of the function $(f_1,f_2,...,f_m)$, it is almost impossible to identify the specific form, let alone to solve the equations. In this case, the function can be turned into the form of a power-series of variables $(x_1,x_2,...,x_n)$ expanded to a certain power order. Then the coefficients of power-series can be calculated through numerical computation method to confirm the power series form of this function. The relationship between $(F_1,F_2,...,F_m)$ and $(x_1,x_2,...,x_n)$ can be established approximately as given below:

$$F_j = F_{0j} + \frac{\partial f_j}{\partial x_1}(x_1 - x_{01}) + \cdots + \frac{\partial f_j}{\partial x_n}(x_n - x_{0n}), \quad (2)$$

where F_{0j} are the residual aberration values of the ideal testing system; $x_i - x_{0i}$, $i = 1,2,...,n$, are the changes of each structural parameter; F_j are measured values of aberrations; $\partial f_j/\partial x_1, \partial f_j/\partial x_2, ..., \partial f_j/\partial x_n$ are the partial derivatives of aberrations with respect to structural parameters. Take the difference quotient $\delta f_j/\delta x_1, \delta f_j/\delta x_2, ..., \delta f_j/\delta x_n$ to replace the differential quotient $\partial f_j/\partial x_1, \partial f_j/\partial x_2, ..., \partial f_j/\partial x_n$. Then the approximate linear equations are established as follows:

$$F_j = F_{0j} + \frac{\delta f_j}{\delta x_1}\Delta x_1 + \cdots + \frac{\delta f_j}{\delta x_n}\Delta x_n. \quad (3)$$

The above equation can be expressed simply by using matrix form.

Suppose

$$\Delta F = \begin{vmatrix} \Delta F_1 \\ \vdots \\ \Delta F_m \end{vmatrix} = \begin{vmatrix} F_1 \\ \vdots \\ F_m \end{vmatrix} - \begin{vmatrix} F_{01} \\ \vdots \\ F_{0m} \end{vmatrix},$$

$$\Delta X = \begin{vmatrix} \Delta x_1 \\ \vdots \\ \Delta x_m \end{vmatrix} = \begin{vmatrix} x_1 \\ \vdots \\ x_m \end{vmatrix} - \begin{vmatrix} x_{01} \\ \vdots \\ x_{0m} \end{vmatrix},$$

$$A = \begin{vmatrix} \frac{\delta f_1}{\delta x_1} & \cdots & \frac{\delta f_1}{\delta x_n} \\ \vdots & \ddots & \vdots \\ \frac{\delta f_m}{\delta x_1} & \cdots & \frac{\delta f_m}{\delta x_n} \end{vmatrix}.$$

Then Eq. (2) can be written as

$$A \cdot \Delta X = \Delta F, \quad (4)$$

where $\Delta X = X - X_0$ is the value of parameter that needs to be adjusted; $\Delta F = F - F_0$, is the difference between the measured aberration and the designed aberration and is determined by the current image quality and the result of designed data; A is the sensitivity matrix, which is determined by the designed data for the testing system.

3 Paraboloidal mirror testing

3.1 Optical path of testing

In order to verify the separation model, a paraboloidal mirror with 600 mm aperture is tested using null compensation method. The testing system layout is shown in Fig. 1. The parallel rays from the interferometer pass through the compensator, and meet the paraboloidal mirror at the ideal positions. The rays reflected by paraboloidal mirror, carrying the surface information of paraboloidal mirror, pass through the compensator again and change into parallel rays after passing through it. These parallel rays interfere with the reference light to get the interference fringes. When the paraboloidal mirror has surface errors, the deformation of fringes shows the surface errors.

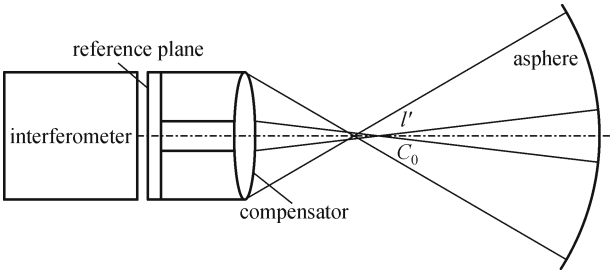

Fig. 1 Diagram of aspheric surface test (C_0: center of curvature of aspheric surface; l': paraxial image distance of compensator)

In this study, an Offner compensator is designed to test the 600 mm paraboloidal mirror. Testing system data is shown in Table 1.

Table 1 Designed data of testing system

	radius/mm	thickness/mm	glass	diameter/mm	conic
0	infinity	infinity	—	0	—
1	205.7026	25	1.514748	100	—
2	infinity	266.9436	—	100	—
3	−93.2908	12	1.514748	50	—
4	−318.103	5008.855	—	56	—
5	−4800	−5008.86	mirror	601.2184	−1
6	−318.103	−12	1.514748	56	—
7	−93.2908	−266.944	—	50	—
8	infinity	−25	1.514748	100	—
9	205.026	−20	—	100	—
10	—	−100	—	92.91437	—

3.2 Structural maladjustment (ΔX)

As shown in Fig. 1, maladjustments may be induced because of the relative position changes among interferometer, compensator and the mirror under test. Each component has six degrees of freedom (three translational degrees of freedom, three rotation degrees of freedom), so the whole testing system has eighteen degrees of freedom. They are not completely independent of each other but incorporated with each other.

First, to facilitate the discussion, the position of interferometer is fixed and it will not be adjusted in the following adjustment. So the six degrees of freedom of interferometer will not participate in the adjustment. Because the maladjustments of interferometer can be compensated by other components, the result will not be affected.

Second, because of the symmetry along the Z-axis of compensator and the mirror under test, the rotation around the Z-axis will not introduce any adjustment error and thence can be ignored.

Lastly, because the incident light to the compensator is a parallel one, the Z-axis will not have any impact on the aberrations, thus need to be ignored.

Therefore, due to the degeneracy of degrees of freedom, eventually, there will only be nine degrees of freedom left. They are: four degrees of freedom of the compensator (the X-, Y-axis decenter, noted as L_{dx}, L_{dy}; the tilt X-, Y-axis, noted as L_{tx}, L_{ty}), five degrees of freedom of the mirror under test (the X-, Y-axis decenter, noted as M_{dx}, M_{dy}; the tilt X-, Y-axis, noted as M_{tx}, M_{ty}; the decenter Z-axis, which is the distance between compensator and the mirror under test, noted as Dis for simplicity).

3.3 Sensitivity matrix (A)

According to Eq. (3), the sensitivity matrix is calculated by replacing the differential quotient $\partial f_j/\partial x_1$,$\partial f_j/\partial x_2$,..., $\partial f_j/\partial x_n$ with the difference quotient $\delta f_j/\delta x_1$,$\delta f_j/\delta x_2$,..., $\delta f_j/\delta x_n$. The matrix is solved according to the ideal testing system's specific structure, before the maladjustments are adjusted. The sensitivity matrix A can evaluate the priority of every degree of freedom. The sensitivity matrix A affects the convergence of adjusting variables, so it is necessary to improve the sensitivity matrix and eliminate related variables in order to prevent the early divergence of variables and accelerate the convergence [6–9].

The tested paraboloidal mirror is of a circular aperture, which is very proper to use Zernike polynomial to fit wave front. At the same time, Zernike polynomials have the property of rotational symmetry and orthogonality on unit circle. And it can establish the relation easily between the polynomial coefficient and Seidel aberration coefficients, which is advantageous and convenient to confirm geometric aberration and separate maladjustments of the testing system. Consequently, we adopt Zernike coefficients as image quality evaluation parameter. The sensitivity matrix is obtained by adopting the following steps.

a) Give a micro-increment ΔX_i to a certain structural parameter of the original system.

b) Then the system aberrations will change and calculate the aberration increment ΔF_i due to the micro-increment ΔX_i.

c) Use Fringe Zernike polynomials (36 terms) fit wavefront and calculate the ratio of the Zernike coefficients and micro-increment ΔX_i. In this way, an element in matrix A is obtained.

d) Recover the changed parameters and repeat the above steps to obtain the other elements of matrix A.

3.4 Analysis of ΔX

The relation between structural maladjustment and aberration is so complicated that it is a little difficult to establish a relationship between them. But some of the relations can be shown approximately by changing the structural parameters of the system, and analyzing the graphical relations between structural maladjustment and aberration. Hereupon, for explanation, an example of compensator rotated along X-, Y- axis is given.

3.4.1 X-axis tilt of compensator (L_{tx})

Non-zero terms include:1,3,4,6,7,9,11,12,14,17,19,22, 24,29; total 14 terms. The terms: 9,11,12,14,17,19,22, 24,29, are so small that they can be considered to be approaching approximately the value of zero. The rest Zernike coefficients of non-zero terms are shown in Fig. 2.

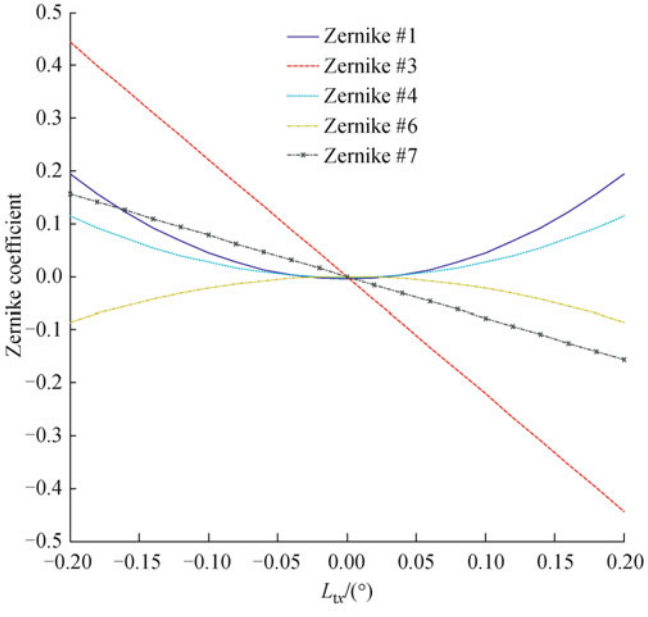

Fig. 2 Zernike coefficients versus L_{tx}

3.4.2 *Y*-axis tilt of compensator (L_{ty})

Non-zero terms include: 1,2,4,6,8,10,11,12,14,16,18,22, 24,30; total 14 terms. The terms: 10,11,12,14,16,18,22,24, 30,nearly approach to zero. The rest of the Zernike coefficients are shown in Fig. 3.

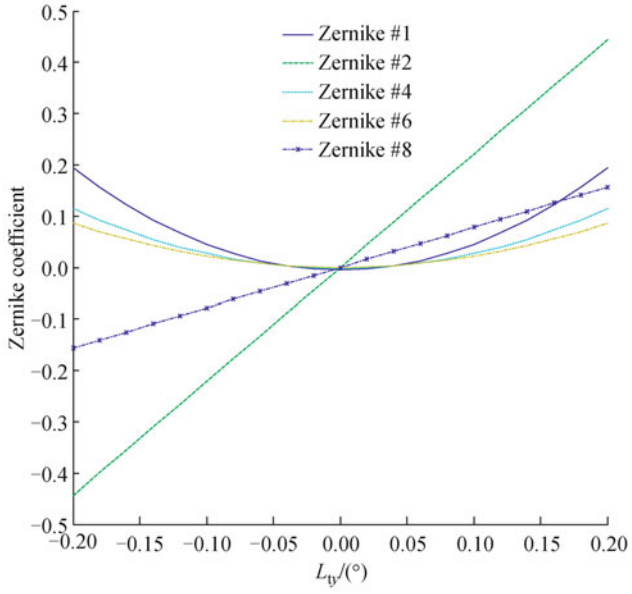

Fig. 3 Zernike coefficients versus L_{ty}

Applying the same method, the curves of Zernike coefficients are available for analysis with some additional degrees of freedom to take into account. According to the curve shown in Figs. 2 and 3, and the relationship between Zernike coefficients and geometric aberrations, a relationship between the structural parameters and the aberrations can be established to an approximate extent.

4 Simulation of adjustment

In the process of simulation of adjustment, first the maladjustments are introduced intentionally and the wavefront aberration is obtained through ZEMAX software. The data is saved into a separate file and the sensitivity matrix is calculated automatically. In the last step, the corresponding maladjustment is solved and then adjusted accordingly.

The actual adjusting mechanism has a certain limit of adjustment accuracy. For example, the displacement accuracy is up to 1.25 μm, the angular displacement is up to 1.125″. In order to simulate the adjustment situation more realistically, the value of each adjustment should be limited to the real precision of the adjusting mechanism and the remainder value should be rounded off. Figure 4

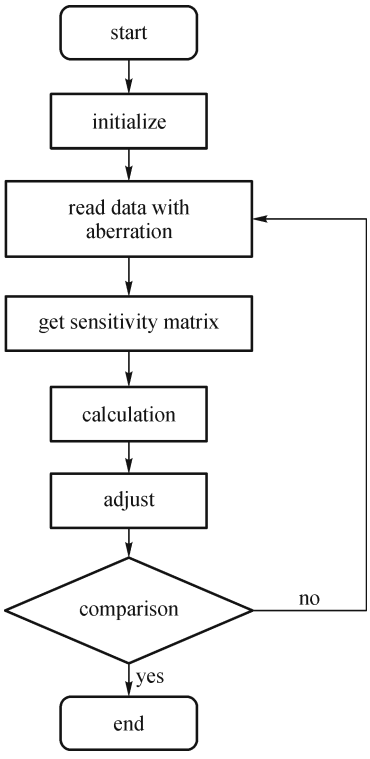

Fig. 4 Flow chart for adjustment program

shows the process of adjustment.

In order to verify the error separation and the results of the adjustment, we introduced nine structural parameters for the maladjustment in this experiment. Figure 5 shows the aberration before and after maladjustment. Figure 6 shows the aberrations during the adjustment. Unit adopted: (λ, λ= 0.6328 μm).

5 Conclusion

According to the analysis of simulation data, after error separation and adjustment for three times, the maladjustment can be figured out and adjusted accordingly. The values PV, RMS have met the designed standards. When compared with manual testing, this method seems to improve the testing precision, reduces the testing time, and also reduces the personnel technological requirements. The error separation model is feasible for other coaxial quadratic aspherical surfaces besides the paraboloidal mirror, but for the test of off-axis aspheric surfaces, further research is needed.

Acknowledgements This work was supported by the National Natural Science Foundation of China (Grant No. 60978043), the Hi-Tech Research and Development Program of China (No. 2009AA04Z115), the Key Lab of Beijing Advanced Manufacturing Technology, and the Beijing Municipal Natural Science Foundation Project (No. 4092036).

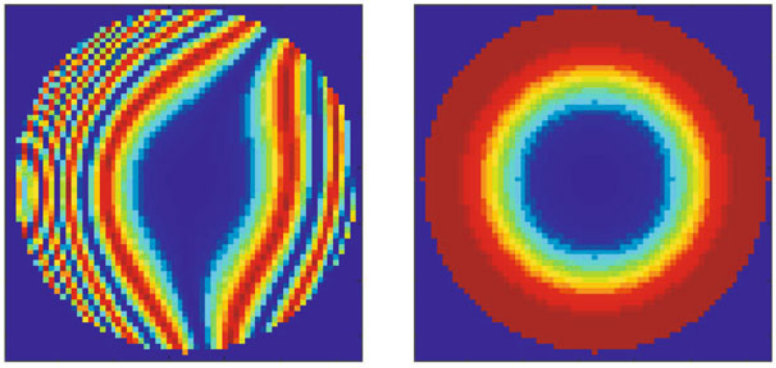

Fig. 5 Comparison of aberrations. (a) With maladjustment (PV = 3.3922, RMS = 0.59348); (b) without maladjustment (PV = 0.007234, RMS = 0.002486)

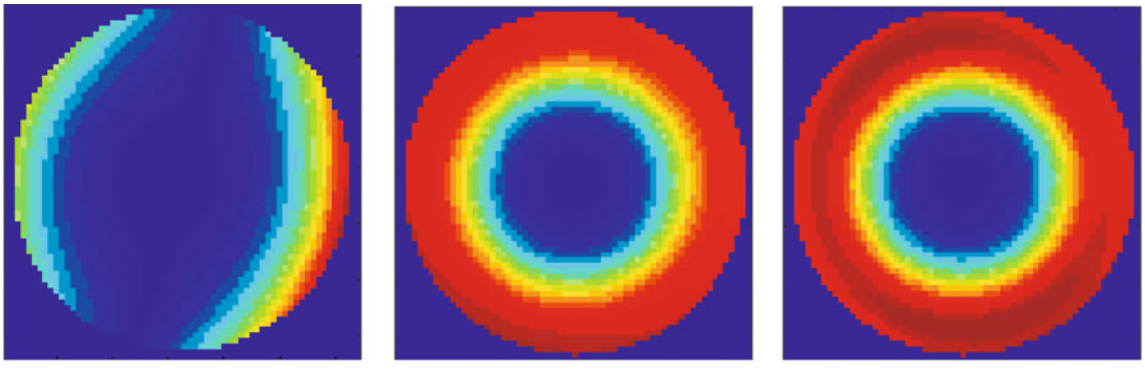

Fig. 6 Process of adjustment. (a) After the first adjustment (PV = 0.15786, RMS = 0.028318); (b) after the second adjustment (PV = 0.008371, RMS = 0.002675); (c) after the third adjustment (PV = 0.007036, RMS = 0.002334)

References

1. Cheng H B. Interferometric null testing and the model for separating adjustment errors. Journal of Harbin Institute of Technology, 2006, 38 (8): 1247–1250 (in Chinese)
2. Nam J, Rubinstein J, Thibos L. Wavelength adjustment using an eye model from aberrometry data. Journal of the Optical Society of America A, 2010, 27(7): 1561–1574
3. Cheng H B, Feng Z J. Error-separation model for interferometric testing aspheric surfaces based on wavefront aberrations. Journal of Tsinghua University, 2006, 46(2): 187–190 (in Chinese)
4. Chen X L, Ruan N J, Ma J, Su Y. Figure analysis and adjustment of a large aperture reflector. In: Proceedings of 4th International Symposium on Advanced Optical Manufacturing and Testing. 2009, 1561–1574
5. Liu J F, Long F N, Zhang W. Study on computer-aided alignment method. Proceedings of SPIE, 2005, 5638: 674–681
6. Lim R S. Staged attitude-metrology pointing control and parametric integrated modeling for space-based optical systems. Dissertation for the Master's Degree. Cambridge: Massachusetts Institute of Technology, 2006, 118–124
7. Li Y. Advanced Optical Manufacture Technology. Beijing: Science Press, 2001, 326–365 (in Chinese)
8. Shannon R R, Wyant J. Applied Optics and Optical Engineering. New York: Academic Press, 1992, 2–53
9. Malacara D. Optical Shop Testing. New York: Wiley-Interscience, 2006, 498–546